time constant τ_{ts_0}. No photoconductivity was observed at room temperature because of the short time constant in absence of traps.

4. Oxygen-Halogen Sensitization

In the case of pretreatment with oxygen followed by halogen treatment, the oxygen electron traps are produced by the oxygen treatment and not removed by baking in vacuum. Sufficient selenium atoms must evaporate from the lattice during the vacuum baking to produce *n*-type material. Then treatment with the halogen lowers the Fermi level and empties the oxygen traps so that they can effectively trap electrons. Appreciable sensitivity is observed at 25°C and −195°C, showing τ_t values of 1 microsecond and 5 milliseconds, respectively.

D. CONCLUSIONS

From an examination of the intrinsic, majority carrier, and minority carrier models of photoconductivity, in terms of an experimental study of the sensitization of PbSe films, we have concluded that oxygen serves the important function of introducing minority carrier traps which are effective at room temperature, and that the photoconductivity is due to a change in the density of majority carriers.

PHYSICAL REVIEW VOLUME 105, NUMBER 6 MARCH 15, 1957

Infrared-Absorption Studies on Barium Titanate and Related Materials*

J. T. LAST†
Laboratory for Insulation Research, Massachusetts Institute of Technology, Cambridge, Massachusetts
(Received November 5, 1956)

The infrared-absorption spectrum of $BaTiO_3$ has been measured for thin single crystals and for powder samples dispersed in pressed KBr disks. Absorption bands for single-crystal samples occur at 495 cm^{-1} and at *ca* 340 cm^{-1}, arising from normal vibrations of the TiO_3 group. A third vibration, a motion of Ba against the TiO_3 group, occurs below the experimentally accessible range. A frequency of about 225 cm^{-1} is expected for this vibration on the basis of a comparison of the specific heat contributions of the observed bands with the measured low-temperature specific heat. Measurements were made on the 495-cm^{-1} band over a wide temperature range. As the crystal changes from the cubic to the tetragonal, orthorhombic, and rhombohedral structures, there occurs band splitting which can be related to the change of crystal symmetry. The spectra of the perovskite titanates, $SrTiO_3$, $PbTiO_3$, and $CaTiO_3$, and the perovskite niobates, $KNbO_3$ and $NaNbO_3$, have been found to be similar, in general features, to that of $BaTiO_3$. The slight differences in band frequency and structure can be related to differences in unit-cell size and symmetry. Integrated band intensities have been found to be in reasonable agreement with measurements on other oxide systems that have vibrations in this spectral region.

INTRODUCTION

STUDIES of the spontaneous orientation of dipole moments in ferroelectrics and ferromagnetics have been carried out at the Laboratory for Insulation Research.[1,2] To investigate the phenomena taking place in such materials as the titanates or ferrites, tools of nondestructive analysis are needed which can give information on atomic arrangements and interatomic forces in the crystal lattice. One of these tools is infrared spectroscopy. A first infrared study of ferrites has recently been carried through in this laboratory[3] and has given promise of locating cations in their oxygen surroundings. The present investigation is a complementary study on ferroelectrics, to establish how the infrared vibrational frequencies, and thus the interatomic forces, are affected by the onset of the ferroelectric state and by the various low-temperature phase transitions. Measurements have been made of the absorption spectra of thin single crystals, the absorption spectra of powdered samples dispersed in pressed potassium bromide disks, and the reflection spectra of thick single crystals.

$BaTiO_3$, in the modification having unusual electrical properties, has a perovskite structure. Above the Curie temperature (~120°C) the lattice has cubic symmetry, with a Ti ion at the center of the unit cell, O ions centered on the six cube faces, and Ba ions on the cube corners (Fig. 1). The structure can be described as a system of TiO_6 octahedra joined at the corners with Ba ions placed in the interstitial positions between the octahedra.

As the cubic crystal is cooled through the Curie point, a polar axis develops along a [100] direction, and the elongation in this direction leads to a structure with tetragonal symmetry. In general, a ferroelectric

* Sponsored by the U. S. Office of Naval Research, the Army Signal Corps, the Air Force, and the Army Ordnance.
† Present address: Shockley Semiconductor Laboratory, Beckman Instruments, Inc., Mountain View, California.
[1] A. von Hippel, Revs. Modern Phys. **22**, 221 (1950).
[2] von Hippel, Westphal, and Miles, Technical Report 97, Laboratory for Insulation Research, Massachusetts Institute of Technology, July, 1955.
[3] R. D. Waldron, Phys. Rev. **99**, 1727 (1955).

domain structure results because the polar axis can develop in several equivalent directions. Near 0°C the polar axis shifts to the [110] direction and at about −70°C to the [111] direction with a structural change to orthorhombic and then to rhombohedral. The material remains ferroelectric throughout.

X-ray measurements of Evans[4] and the neutron diffraction measurements of Frazer *et al.*[5] indicate that the Ti ion in tetragonal $BaTiO_3$ is displaced to an off-center position in the TiO_6 octahedron. The two Ti-O distances along the polar axis are 1.87 and 2.17 A, compared to the Ti-O distance of 1.997 A at right angles to the polar axis.

Previous single-crystal absorption measurements on $BaTiO_3$ have been confined to the near infrared. Measurements by Hilsum[6] indicated a weak absorption band at 1200 cm^{-1}, shouldered on a strong absorption band beginning at about 1400 cm^{-1} and continuing to a point of zero transmission at about 850 cm^{-1}. Measurements by Mara *et al.*[7] on powder samples of $BaTiO_3$ dispersed on a KBr plate showed a strong band centered at 550 cm^{-1}, and a second band starting near 450 cm^{-1} and reaching a point of maximum absorption beyond 300 cm^{-1}.

INSTRUMENTATION AND SAMPLE PREPARATION

The spectra measured in this investigation were recorded with a Beckman IR-3 spectrophotometer, equipped with CaF_2, KBr, and KRS-5 prisms, that provided an operating range extending from the visible to about 300 cm^{-1}. The instrument was calibrated by recording the spectra of gases which have been measured with considerable accuracy on grating instruments.[8]

A Dewar microcell, designed in this laboratory by R. D. Waldron, was used to investigate the spectra of small single crystals between −190° and +175°C. The slit image was reduced at a ratio of about 15 to 1 by

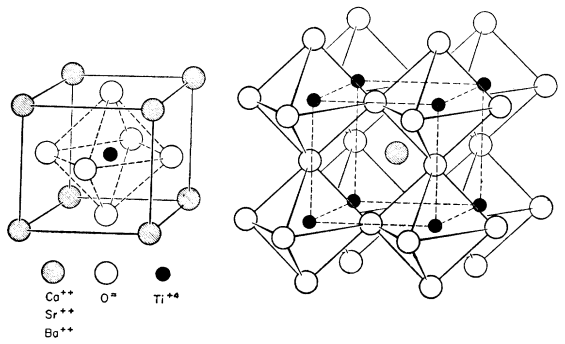

FIG. 1. The ideal perovskite structure.

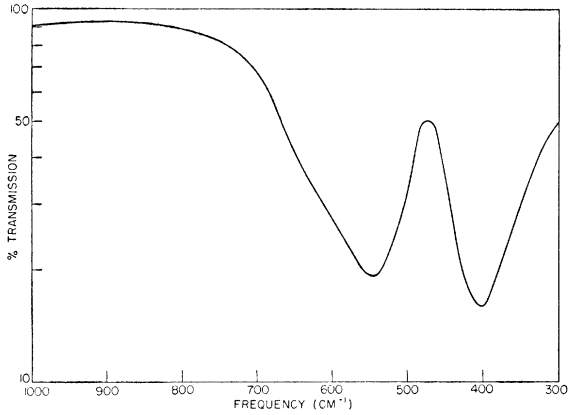

FIG. 2. The infrared-absorption spectrum of powdered $BaTiO_3$ (0.57 mg/cm²) dispersed in a pressed KBr disk.

the use of parabolic KBr and KRS-5 lenses, permitting the measurement of samples as small as 1×0.5 mm. For the investigation of the low-temperature spectra of pressed disks and large samples, a Dewar cell with AgCl and KRS-5 windows was used, similar in design to that described by Wagner and Hornig.[9] A three-mirror reflection device was used for the measurement of the reflection spectra of thick single crystals.

Single crystals of $BaTiO_3$, about 1.5 μ thick, thin enough to transmit a measurable quantity of light in the absorption band, were prepared by etching in hot phosphoric acid.[10] The crystals, of an original thickness of about 100 μ, were etched in acid heated above the Curie temperature to prevent the selective etching of domains.

Crystals prepared by this etching technique were sufficiently plane-parallel to permit the observation of interference bands in the near infrared. An accurate value of the crystal thickness could be obtained from the frequency separation of these bands and the known value of the index of refraction.

In order to measure the spectra for materials for which thin single crystals could not be obtained, pressed-disk samples were prepared by the technique of Stimson[11] and Schiedt.[12] A small section of a single crystal was powdered to a particle size of about one micron, and a few milligrams of the powder mixed with powdered KBr and then pressed in a cylindrical die. This resulted in clear disks which could be used to 300 cm^{-1}.

EXPERIMENTAL RESULTS

Absorption Spectrum of $BaTiO_3$

Measurements on the absorption spectrum of $BaTiO_3$ in the region from 1000 to 300 cm^{-1}, where the trans-

[4] H. T. Evans, Jr., Technical Report 58, Laboratory for Insulation Research, Massachusetts Institute of Technology, January, 1953.
[5] Frazer, Danner, and Pepinsky, Phys. Rev. **100**, 745 (1955).
[6] C. Hilsum, J. Opt. Soc. Am. **45**, 771 (1955).
[7] Mara, Sutherland, and Tyrell, Phys. Rev. **96**, 801 (1954).
[8] Downie, Magoon, Purcell, and Crawford, J. Opt. Soc. Am. **43**, 941 (1953).
[9] E. L. Wagner and D. F. Hornig, J. Chem. Phys. **18**, 296 (1950).
[10] J. T. Last, Rev. Sci. Instr. (to be published).
[11] M. M. Stimson and M. J. O'Donnell, J. Am. Chem. Soc. **74**, 1805 (1952).
[12] U. Schiedt and H. Reinwein, Z. Naturforsch. **7B**, 270 (1952); Appl. Spectroscopy **7**, 75 (1953).

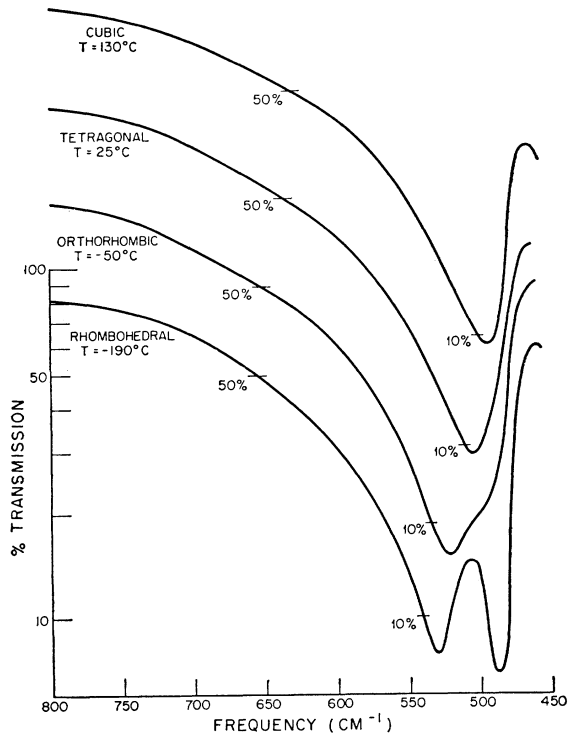

FIG. 3. The infrared-absorption spectra of single-crystal $BaTiO_3$ (1.5 μ thick) for the cubic, tetragonal, orthorhombic, and rhombohedral phases.

mission of thick single crystals is extremely low, were made on powder samples dispersed in pressed KBr disks. Two absorption bands were observed (Fig. 2). The higher frequency band, ν_1, extends from about 800 to 475 cm^{-1}, with a center of 540 cm^{-1}. This band is asymmetric, with a high-frequency tail, and has a band half-width of about 165 cm^{-1}. The lower frequency band, ν_2, extends from about 475 cm^{-1} to the limit of the available experimental range at about 300 cm^{-1}, with a center at 400 cm^{-1} and a half-width of about 120 cm^{-1}. No change was observed in ν_2 in the temperature range from $+150°$ to $-150°C$, covering the four crystal phases; band ν_1 becomes doubled at low temperatures.

Since the phase transitions in the powder samples cover a wide temperature range, the effect of the change in crystal symmetry was investigated in greater detail, using single crystals in the variable-temperature microcell. In order to transmit a measurable amount of energy through the crystal, crystals of 1.5-μ thickness were required. These measurements could be carried out only to 400 cm^{-1}, because of the lack of sufficient radiant energy at lower frequencies. Only the higher frequency band ν_1 could therefore be observed.

In single-crystal, cubic $BaTiO_3$ ($T > 115°C$), band ν_1 is centered at 495 cm^{-1} (Fig. 3). When the temperature was lowered below the Curie point and the crystal became tetragonal, this band became slightly broader and the location of the band center depended on the domain arrangement. For a "c" plate, with the polar "c" axis normal to the crystal face, the band was centered at 495 cm^{-1}. For a mixed-domain crystal, the center lay between 495 and 510 cm^{-1}, depending on the particular domain configuration.

Room-temperature measurements were carried out to observe the difference in vibrational frequency along the polar ("c") axis and at right angles thereto ("a" axis). The spectra measured with polarized infrared radiation (AgCl sheet polarizer) are shown in Fig. 4. The band is centered at 495 and 517 cm^{-1} for the electric vector parallel to the "a" axis and to the "c" axis, respectively. The intensities of the two bands were approximately the same.

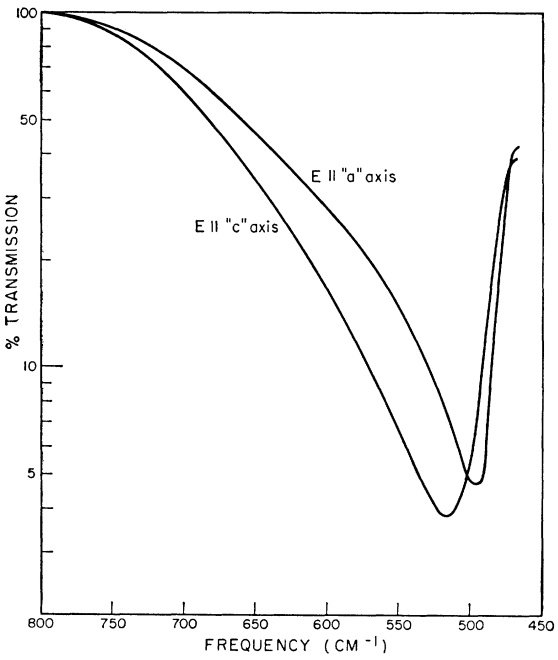

FIG. 4. The polarized, infrared-absorption spectra of tetragonal single-crystal $BaTiO_3$ (1.5 μ thick) along the "c" and "a" axes.

In the temperature range from $0°$ to $-70°C$, where the crystal is orthorhombic, the band is centered at 520 cm^{-1}, with a shoulder at 495 cm^{-1} (Fig. 3). In the rhombohedral phase, below $-70°C$, the band becomes doubled, with centers at 530 and 490 cm^{-1}. Because of the complex domain configurations of the crystals in these two lower phases, it was not possible to make polarized-light measurements.

In order to observe any possible absorption anomalies in the immediate vicinities of the three phase transitions, the spectrophotometer monochromator was set at a frequency near the band center and the temperature was changed slowly through the transition point. Aside from the slight intensity jumps caused by the shift of band centers at the transition temperatures, no intensity changes were observed.

Hexagonal $BaTiO_3$

In addition to the perovskite modification of $BaTiO_3$, where the TiO_6 octahedra are joined at corners, a hexagonal modification exists, in which two-thirds of the octahedra occur in pairs which share a face to form Ti_2O_9 coordination groups.[13] This modification is not ferroelectric, and no phase transitions have been reported.

The absorption spectrum of a pressed-disk sample of hexagonal $BaTiO_3$, measured at room temperature and at $-150°C$, is shown in Fig. 5. Bands similar in general features to the bands in the perovskite modification but exhibiting additional fine structure are observed. Apart from some sharpening of the band at low temperature, no difference occurs between the room-temperature and low-temperature spectra, in contrast to that found in the case of the perovskite form.

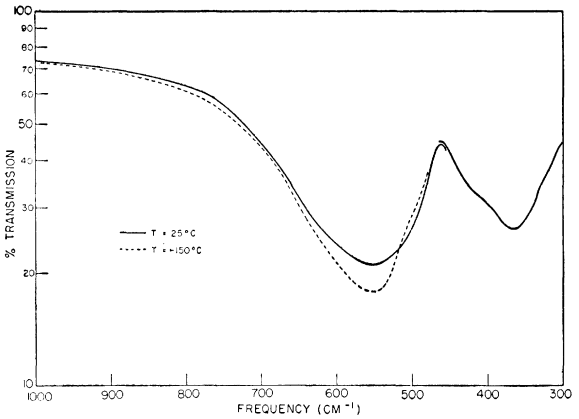

FIG. 5. The infrared-absorption spectrum of powdered hexagonal $BaTiO_3$.

Effect of Cation Replacement

The spectra of several titanates related to $BaTiO_3$ by cation replacement were investigated: the perovskite titanates, $PbTiO_3$, $SrTiO_3$, and $CaTiO_3$, which at room temperature are tetragonal, cubic, and orthorhombic, respectively, and the ilmenite titanates, $CdTiO_3$, $ZnTiO_3$, and $MgTiO_3$.

Figure 6 shows measurements on pressed-disk samples of $PbTiO_3$ and $SrTiO_3$, together with the corresponding spectrum of $BaTiO_3$. The spectra are all similar in general features, with band ν_1 shifted to somewhat higher frequencies in the $PbTiO_3$ and $SrTiO_3$ samples. The bands in $PbTiO_3$ and $SrTiO_3$ sharpened slightly, but exhibited no additional fine structure at low temperatures.

The reflection spectra of these three materials were measured on thick single crystals. Broad bands were observed at frequencies slightly higher than the corresponding absorption bands (Fig. 7).

[13] R. D. Burbank and H. T. Evans, Jr., Acta Cryst. **1**, 330 (1948).

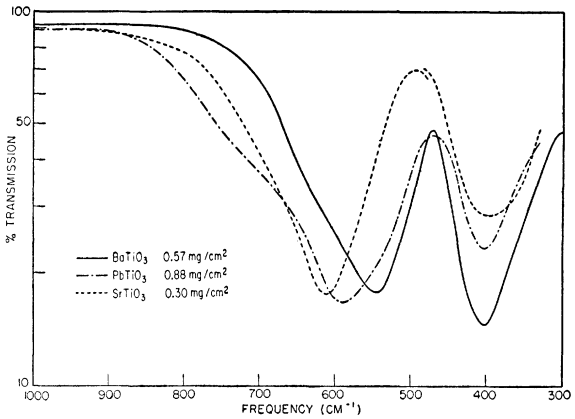

FIG. 6. The infrared-absorption spectra of powdered $BaTiO_3$, $SrTiO_3$, and $PbTiO_3$.

The spectrum of thin, single-crystal $PbTiO_3$, prepared by the etching techniques used on $BaTiO_3$, showed band ν_1 centered at 535 cm^{-1}, with a shoulder at 610 cm^{-1} (Fig. 8). The crystals were too fragile to permit the measurement of the spectrum at low temperatures.

The spectrum of a pressed-disk sample of $CaTiO_3$ has the same general features as that of $BaTiO_3$ (Fig. 9); fine structure appears, caused by the lowered symmetry of this material and by the presence of unreacted material in the powder used.

The three ilmenite titanates, $CdTiO_3$, $ZnTiO_3$, and $MgTiO_3$, show a high-frequency band, broader and less distinct than the band in the perovskite form (Figs. 9 and 10). The low-frequency band is doubled.

The location of the band centers of all materials measured in this investigation are shown in Table I.

$KNbO_3$ and $NaNbO_3$

$KNbO_3$ and $NaNbO_3$, with a perovskite structure similar to $BaTiO_3$, have high-temperature Curie points, several high-temperature structural transitions, and are

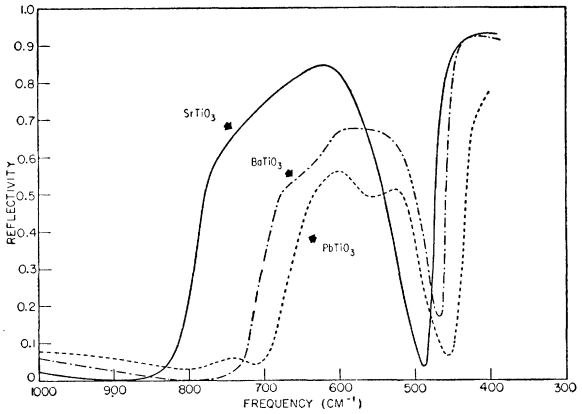

FIG. 7. The infrared-reflection spectra of single-crystal $BaTiO_3$, $SrTiO_3$, and $PbTiO_3$.

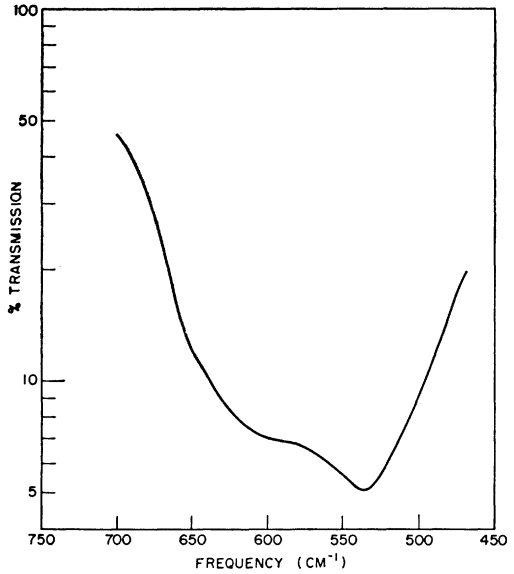

FIG. 8. The infrared-absorption spectrum of single-crystal $PbTiO_3$ (2 μ thick).

orthorhombic at room temperature.[14–16] $KNbO_3$ is ferroelectric at room temperature and has a transition to a rhombohedral phase at about $-50°C$, showing pronounced thermal hysteresis. $NaNbO_3$, antiferroelectric at room temperature, has a transition to a ferroelectric state at about $-200°C$, again with a large thermal hysteresis.

The spectra of pressed-powder disks of $KNbO_3$ and $NaNbO_3$, prepared from powdered crystal sections of single crystals (Fig. 11) are similar to that of orthorhombic $BaTiO_3$, with a shoulder on the low-frequency side of band ν_1. The band centers in $KNbO_3$ are located at 660, 550 (shoulder), and 375 cm^{-1}; in $NaNbO_3$ at 675, 510 (shoulder), and 375 cm^{-1}. Little difference was observed between the room-temperature and low-temperature spectra.

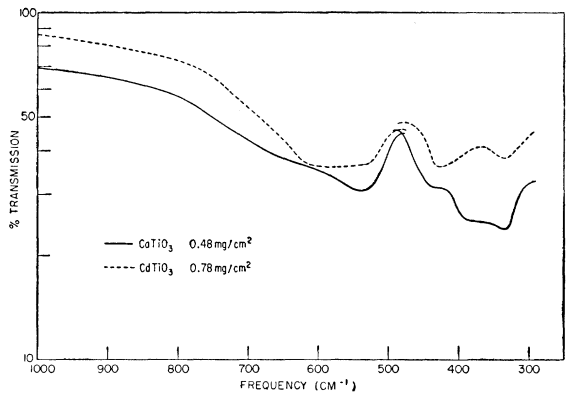

FIG. 9. The infrared-absorption spectra of powdered $CaTiO_3$ and $CdTiO_3$.

[14] E. A. Wood, Acta Cryst. **4**, 353 (1951).
[15] Shirane, Danner, Pavlovik, and Pepinsky, Phys. Rev. **93**, 672 (1954).
[16] Shirane, Newnham, and Pepinsky, Phys. Rev. **96**, 581 (1954).

Effect of Disk Matrix Material

In order to investigate the dependence of the shape and location of the absorption spectrum of powdered $BaTiO_3$ on the optical properties of the material in which it is dispersed, identical $BaTiO_3$ samples were dispersed in matrices of increasing indexes of refraction: KBr, AgCl, TlCl, and TlBr.

The centers of the absorption bands shift to lower frequencies when materials of higher index are used (Table II).

DISCUSSION

Thin-Crystal and Pressed-Disk Transmission

The observed transmission curve of thin single crystals is a combination of beam-attenuation effects due to crystal absorption and to reflection from the crystal surfaces. Using single-surface reflectivity measurements, the position of the true transmission minimum can be determined by treating the limiting cases of constructive and destructive interference in the reflected waves. In the case of thin single crystals of $BaTiO_3$, the surface reflectivity has a very slight effect on the transmission minimum; correcting for this effect shifts band ν_1 about 10 cm^{-1} toward lower frequencies.

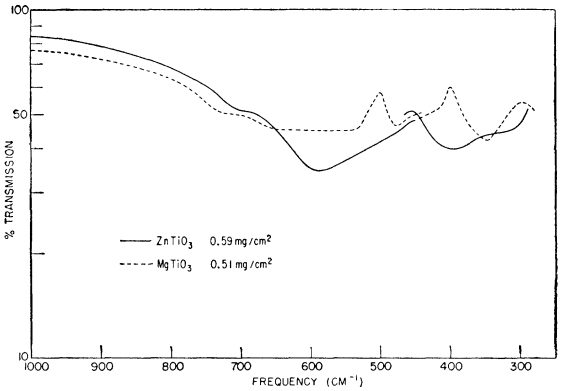

FIG. 10. The infrared-absorption spectra of powdered $MgTiO_3$ and $ZnTiO_3$.

For the case of the pressed-powder samples, it has been observed that the absorption bands shift to lower frequency when the index of refraction, and thus the atomic polarizability, of the disk matrix is increased. Although a quantitative discussion of this shift cannot be carried out because of the difficulty of evaluating the local field accurately, it can be noted that the observed shift is in the direction expected, considering simple electrostatic interactions.

Since it has not been possible to measure the absorption maximum of band ν_2 for single crystals corresponding to the pressed-disk band at 400 cm^{-1}, the

frequency of this band has been estimated from the shift between single-crystal and pressed-disk frequencies for the higher frequency band ν_1. This band is located at 540 cm^{-1} for a pressed-disk sample, and at 495 cm^{-1} for a single crystal corrected for surface reflectivity. The pressed-disk frequency is lowered by about 15 cm^{-1} when the higher-index powder TlCl is substituted for KBr.

For band ν_2 the KBr pressed-disk frequency is shifted about 40 cm^{-1} toward lower frequencies when a TlCl matrix is used. A value of 340 cm^{-1} has been chosen for the single-crystal vibrational frequency, based on these powder shifts and on expected band half-widths. This value is probably accurate to within 25 cm^{-1}.

Normal Vibrations of the Perovskite Lattice

An extensive body of theoretical and experimental evidence indicates that the absorption bands in the infrared spectra of solids are caused by excitation of optically active vibrations. In order to interpret these spectra, we can study the vibrations as wave motions in periodic structures. In this section we shall qualitatively develop the complete vibrational spectrum of a cubic perovskite crystal, and indicate the requirements for modes which can be excited by infrared radiation. The general form of the infrared vibrations can be determined by the use of lattice-symmetry arguments.

TABLE I. Absorption-band centers.

	ν_1 cm^{-1}	ν_2 cm^{-1}
Single-crystal spectra		
$BaTiO_3$ (cubic)	495	
$BaTiO_3$ (tetragonal)	517; 495	
$BaTiO_3$ (orthorhombic)	520; 495 (shoulder)	
$BaTiO_3$ (rhombohedral)	532; 490	
$PbTiO_3$ (tetragonal)	610 (shoulder); 535	
Pressed-disk spectra		
$BaTiO_3$ (tetragonal)	545	400
$BaTiO_3$ (hexagonal)	555	365
$PbTiO_3$ (tetragonal)	590	405
$SrTiO_3$ (cubic)	610	395
$CaTiO_3$ (orthorhombic)	540; 700 (shoulder)	360 (broad)
$KNbO_3$ (orthorhombic)	660; 550 (shoulder)	375
$NaNbO_3$ (orthorhombic)	675; 510 (shoulder)	375
$CdTiO_3$ (ilmenite)	575 (broad)	425; 335
$ZnTiO_3$ (ilmenite)	590 (broad)	400; 315 (shoulder)
$MgTiO_3$ (ilmenite)	600 (broad)	475; 350

A crystal of $BaTiO_3$ containing N unit cells, each with 5 atoms, has $15N$ degrees of freedom. Of these $15N$ modes, there are $3N$ degrees of freedom related to translational motion and $3N$ to torsional motion of the unit cell. The remaining $9N$ modes are associated with vibrational degrees of freedom.

In the Born-von Kármán treatment of lattice vibrations,[17] it is shown that each normal mode of a unit cell corresponds to N normal modes of the crystal, the wavelength associated with the lattice vibration determining the phase shift between adjacent unit cells. In the case of optically active vibrations, the phase of the lattice vibration must match that of the exciting electromagnetic wave. Since the unit-cell dimensions are extremely small compared to the exciting infrared wavelength, the phase shift between neighboring cells is negligible and all equivalent atoms in the lattice can be considered to vibrate in phase. A discussion of the vibrational frequencies of the unit cell will thus give information equivalent to one of the vibrational frequencies of the complete lattice.

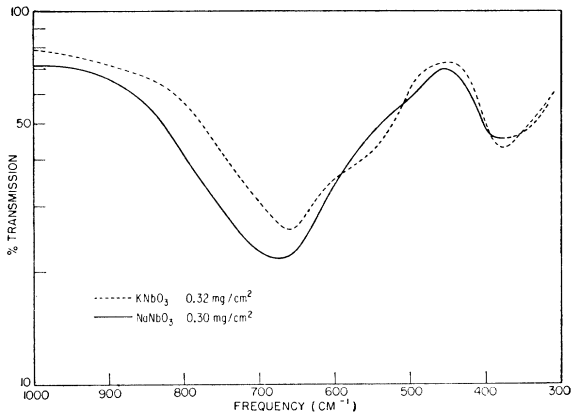

FIG. 11. The infrared-absorption spectra of powdered $KNbO_3$ and $NaNbO_3$.

The nine vibrations of the unit cell can be classified by division into three vibrations of Ba against the TiO_3 group, and six internal TiO_3 vibrations. The interactions between these motions depend upon the masses and restoring forces of the vibrating atoms, and can be expected to be small in the case of $BaTiO_3$. The Ba-(TiO_3) vibrations can be treated by considering the TiO_3 group as a single atom situated at the Ti position, and the vibrational problem that of a diatomic crystal of equivalent structure (e.g., the CsCl structure). In the cubic phase, this will lead to a triply degenerate vibration since three equivalent axes exist.

In discussing the vibrational nature of the TiO_3 group, it is considered to be arranged as a central Ti atom octahedrally surrounded by six O half-atoms, to give the group the correct symmetry properties. This octahedron has the symmetry of the point group O_h, which has the six species of normal vibrations, A_{1g}, E_g, F_{1u}, F_{1u}, F_{2u}, F_{2g}, as discussed by Herzberg.[18]

TABLE II. Powder absorption-band centers in $BaTiO_3$.

Disk material	Index of refraction (540 cm^{-1})	Absorption maxima cm^{-1}
KBr	1.48	545; 400
AgCl	1.92	540; 380
TlCl	2.06	532; 365
TlBr	2.25	535; 360

[17] M. Born and T. von Kármán, Physik. Z. **13**, 297 (1912); **14**, 15 (1913).

[18] G. Herzberg, *Infrared and Raman Spectra* (D. Van Nostrand Company, Inc., New York, 1945), pp. 121 ff.

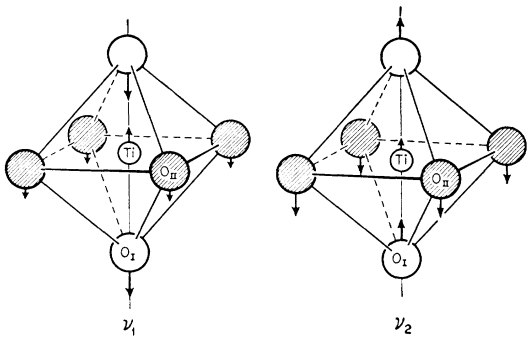

FIG. 12. Schematic infrared-active normal vibrations of a TiO_6 octahedron; ν_1; higher-frequency "stretching" vibration; ν_2: lower-frequency "bending" vibration.

The requirement that atoms in equivalent positions in neighboring cells must perform the same vibrational motion reduces this set of normal vibrations to the two infrared-active vibrations of the species F_{1u}. The infrared-inactive vibrations of species F_{2u} are related to the torsional motion of the unit cell.

If we choose a vertical axis through a Ti-O chain, and label the two O half-atoms lying along this chain O_I and the four O half-atoms at right angles to this axis O_{II}, we can illustrate the two F_{1u} normal vibrations as shown in Fig. 12. In the first, a "stretching" vibration, the motion is primarily that of a change in length of the Ti—O_I bond; in the second, a "bending" vibration, that of a change in the O_{II}—Ti—O_I bond angle. Both the relative magnitude and sign of the displacements will depend on the bond-force constants and relative masses of the atoms. Since three equivalent axes exist in the case of the cubic lattice, these vibrations will be also triply degenerate.

The degree of degeneracy of these two bands in structures of lower symmetry may be determined by resolving the symmetry types of the cubic point group into point groups of lower symmetry, as shown in Table III. The cubic triple degeneracy is partially removed in the tetragonal structure and each of the bands is doubled. In the orthorhombic structure the degeneracy is completely removed and each band is tripled. The symmetry species present in the rhombohedral structure are the same as those of the tetragonal structure and the bands are again doubled. We thus expect three triply degenerate infrared-active vibration bands in the spectrum of cubic barium titanate, with the degeneracies partially or completely removed in the phases of lower symmetry.

Infrared absorption bands have been observed in the vicinity of 500 to 600 cm^{-1} and 350 to 400 cm^{-1} for the various titanates investigated (Table I). The higher frequency band ν_1 will be assigned to the Ti—O_I "stretching" normal vibration [Fig. 12(a)] and the lower band ν_2 to the Ti—O_{II} "bending" normal vibration [Fig. 12(b)]. The stretching vibration is expected to occur at frequencies higher than the bending vibration, from a comparison of the change in potential energy due to repulsive forces between ions in the two normal vibrations. A low-frequency band ν_3, at frequencies below the available experimental range, will be assigned to the cation-(TiO_3) vibration.

Force Constants

Two interatomic force constants can be determined for the various perovskites investigated from the two measured vibrational frequencies ν_1 and ν_2, by the usual normal coordinate treatment. In the present case, the potential energy U is assumed to have the form

$$U=\tfrac{1}{2}\sum k_s q_s^2+\tfrac{1}{2}\sum k_b q_b^2,$$

where $q_s=\Delta z_{\mathrm{Ti}}-\Delta z_{\mathrm{O\ I}}$ and $q_b=\Delta z_{\mathrm{Ti}}-\Delta z_{\mathrm{O\ II}}$, and where z is the atomic coordinate in the Ti—O_I direction, and k_s and k_b are the corresponding force constants. The use of this potential function amounts to treating the vibrations of the TiO_3 group separately from the Ba—(TiO_3) vibrations. This approximation is justified in the present case since little interaction occurs between these two sets of vibrations.

TABLE III. Crystal symmetry and rearrangement of symmetry species for the four phases of $BaTiO_3$.

Symmetry	Point group	Species	Expected band structure
Cubic	O_h	F_{1u}	Single
Tetragonal	C_{4v}	E A_1	Double
Orthorhombic	C_{2v}	B_1 B_2 A_1	Triple
Rhombohedral	C_{3v}	E A_1	Double

The force constants k_s and k_b for the normal vibrations may be obtained by solving the secular equation:

$$\begin{vmatrix}(\mu_0+\mu_1)(2k_s)-\lambda & -\mu_0(4k_b)\\ -\mu_0(2k_s) & (\mu_0+\mu_2)(4k_b)-\lambda\end{vmatrix}=0,$$

where μ_0, μ_1, and μ_2 are the reciprocal masses of Ti, O_I, and O_{II}, respectively, and $\lambda=(2\pi\nu)^2$.

If we call $A=\mu_0+\mu_1$, $B=\mu_0+\mu_2$, $D=\mu_0\mu_1+\mu_0\mu_2+\mu_1\mu_2$, and the two observed frequencies $\lambda_1^{\frac{1}{2}}/2\pi$ and $\lambda_2^{\frac{1}{2}}/2\pi$, we obtain

$$k_s=\left(\frac{\lambda_1+\lambda_2}{4A}\right)\left[1+\left(1-\frac{4BA}{D}\frac{\lambda_1\lambda_2}{(\lambda_1+\lambda_2)^2}\right)^{\frac{1}{2}}\right];$$

$$k_b=\left(\frac{\lambda_1+\lambda_2}{8B}\right)\left[1-\left(1-\frac{4BA}{D}\frac{\lambda_1\lambda_2}{(\lambda_1+\lambda_2)^2}\right)^{\frac{1}{2}}\right].$$

Force constants determined for $BaTiO_3$, $SrTiO_3$, $PbTiO_3$, $KNbO_3$, and $NaNbO_3$, by using the powder-sample frequencies of Table I, and for single-crystal $BaTiO_3$, by using frequencies of 495 and 340 cm^{-1}, are shown in Table IV. In these calculations, the slight

departure from cubic structure which occurs in all materials except $SrTiO_3$ has been neglected.

For the force constants for $BaTiO_3$ computed from the two sets of data, the stretching-force constant is about 5% lower for the single-crystal data than for the powder data, and the bending-force constant is about 30% lower. The force constants computed for the other materials, for which only powder data are available, are probably also somewhat higher than those corresponding to single-crystal frequencies.

Specific Heats

A comparison of the measured low-temperature specific heat of $BaTiO_3$ with that computed from the sum of the Einstein and Debye specific-heat contributions of the various optical and acoustic vibrations lends confirmation to the Ti—O vibrational assignments for ν_1 and ν_2, and may be used to determine the low-frequency vibration ν_3 more accurately.

As discussed earlier, the 15 degrees of freedom of the $BaTiO_3$ unit cell can be separated into three degrees associated with lattice translations, three with infrared-inactive torsional vibrations of species F_{2u}, and three with each of the three infrared-active vibrations. The translational modes will introduce a Debye contribution to the specific heat; the others will be treated as Einstein contributions.

TABLE IV. Computed force constants.

	k_a dynes cm^{-1}	k_b dynes cm^{-1}
$BaTiO_3$ (single crystal)	0.753×10^5	0.417×10^5
$BaTiO_3$ (powder)	0.798×10^5	0.638×10^5 [a]
$SrTiO_3$ (powder)	1.16×10^5	0.561×10^5
$PbTiO_3$ (powder)	1.04×10^5	0.602×10^5
$KNbO_3$ (powder)	1.72×10^5	0.521×10^5
$NaNbO_3$ (powder)	1.80×10^5	0.521×10^5

[a] The force constants for the $BaTiO_3$ powder sample are slightly imaginary for the observed frequencies. Neglecting this very small imaginary part leads to the listed force constants and to frequencies separated by about 5 cm^{-1} more than the observed frequencies.

The two measured vibrations $\nu_1=495$ cm^{-1} and $\nu_2=340$ cm^{-1} have Einstein temperatures of 720° and 490°K. The torsional vibration has a motion similar to that of the infrared-active "bending" vibration ν_2; the Einstein temperatures of these two vibrations will be assumed to be the same. The ratio of the frequency of the Ba—(TiO_3) vibration ν_3 to the limiting translational frequency can be estimated by considering the TiO_3 group to be a single atom, and the Ba—(TiO_3) crystal as a diatomic lattice having the CsCl structure. The infrared-active frequency of this lattice, the same as that of a one-dimensional diatomic chain, is[19]

$$\nu_{\text{opt}}=\frac{1}{2\pi}\left[\frac{M+m}{Mm}(2k)\right]^{\frac{1}{2}},$$

and the maximum translational frequency

$$\nu_{\text{acoust}}=(1/2\pi)(2k/M)^{\frac{1}{2}},$$

where $M>m$, and k is the force constant associated with the vibration. In the present case, the ratio of the two frequencies is

$$\frac{\nu_{\text{acoust}}}{\nu_{\text{opt}}}=\left(\frac{m(TiO_3)}{m(TiO_3)+M(Ba)}\right)^{\frac{1}{2}}=0.64.$$

The molar specific heat under these assumptions is

$$C_v=3R\left[f_E\left(\frac{T}{720}\right)+2f_E\left(\frac{T}{490}\right)+f_E\left(\frac{T}{T_3}\right)+f_D\left(\frac{T}{0.64T_3}\right)\right].$$

The Einstein temperature T_3 for the vibration ν_3 which will lead to an agreement with experimental values of the specific heat[20] can thus be determined.

The measured C_p values may be converted to C_v values by using the thermal expansion coefficients given by Rhodes,[21] and values for the compressibility may be computed from the elastic-constant data of Bond, Mason, and McSkimin.[22] This small C_p-C_v correction, assumed to be linear with temperature, is $0.0014\,T$.

The values of the Einstein temperature for the vibration ν_3 computed on this basis are shown in Table V. The Einstein temperature best fitting the low-temperature data is about 320°K, corresponding to a vibrational frequency of 225 cm^{-1}. Using the one-dimensional diatomic-lattice approximation, this leads to a force constant $k_3=0.84\times10^5$ dynes/cm for the Ba—(TiO_3) vibration. When referred to the CsCl arrangement, k_3 is related to the change in separation of a plane of Ba atoms on the unit-cell face and the TiO_3 group at the center of the unit cell, directed along a [100] or equivalent direction. The force constant

TABLE V. Specific-heat contributions of the $BaTiO_3$ lattice vibrations.

Temp. °K	C_p[20]	C_v[a]	$f_E\left(\frac{T}{720}\right)$	$2f_E\left(\frac{T}{490}\right)$	$f(T_3)$[b]	T_3 °K	ν_3 cm^{-1}
55	4.19	4.12	0.002	0.13	4.0	312	220
75	7.0	6.9	0.04	0.76	6.1	304	210
100	10.3	10.2	0.23	2.20	7.8	312	220
125	13.3	13.1	0.63	3.80	8.7	328	230
150	16.0	15.8	1.14	5.30	9.4	335	235
175	18.2	18.0	1.70	6.48	9.8	351	245

[a] A correction $C_p-C_v=0.0014T$ has been assumed.

[b] $f(T_3)=f_E\left(\frac{T}{T_3}\right)+f_D\left(\frac{T}{0.64T_3}\right)$.

[19] C. Kittel, *Introduction to Solid-State Physics* (John Wiley and Sons, Inc., New York, 1953), pp. 65 ff.

[20] S. S. Todd and R. E. Lorenson, J. Am. Chem. Soc. **74**, 2043 (1952).

[21] R. G. Rhodes, Acta Cryst. **4**, 105 (1951).

[22] Bond, Mason, and McSkimin, Phys. Rev. **82**, 442 (1951).

$k_t = 0.63\times10^5$ dynes/cm for a Ba$-$(TiO_3) bond directed along a cube body diagonal is $\frac{3}{4}$ as large as k_s, since there are eight bonds involved instead of six.

Compressibility and Elastic Constants

Considering $BaTiO_3$ as cubic, one can compute the compressibility from the stretching-force constants k_s for the Ti$-$O bond and k_t for the Ba$-$(TiO_3) bond. For unit contraction along the three axes of the unit cell, six Ti$-$O bonds are each shortened a distance $\frac{1}{2}$, and eight Ba$-$(TiO_3) bonds are each shortened a distance $\sqrt{3}/2$. The energy for unit compression is thus

$$U=\tfrac{3}{4}k_s+3k_t.$$

The energy density of a compressed crystal may be expressed in terms of the elastic constants c_{ij} and the strain and shear components α_i by[23]

$$\tilde{U}=\tfrac{1}{2}\sum_{i,j=1}^{6} c_{ij}\alpha_i\alpha_j.$$

For unit compression of a cubic unit cell of edge length L, this becomes

$$U=\tilde{U}L^3=\tfrac{3}{2}L(c_{11}+2c_{12}),$$

since $\alpha_i^2=1/L^2$. The elastic constants may be replaced by the cubic compressibility through $\beta=3/(c_{11}+2c_{12})$. The compressibility in terms of the force constants for $BaTiO_3$ is therefore $\beta=6L/(k_s+4k_t)$.

Using values $k_s=0.75\times10^5$ dynes/cm, $k_t=0.63\times10^5$ dynes/cm, and $L=4.0\times10^{-8}$ cm, the compressibility $\beta=7.3\times10^{-13}$ cm^2/dyne. This can be compared with a value for the compressibility of 6.17×10^{-13} cm^2 dyne, computed from the elastic constant data determined for single-crystal $BaTiO_3$[22] ($c_{11}=2.06\times10^{12}$ dynes/cm^2; $c_{12}=1.40\times10^{12}$ dynes/cm^2). The agreement is reasonable, considering the potential approximations used and the assumption of cubic symmetry.

A value for the elastic constant c_{11} may be determined directly from the stretching-force constants. For a unit linear contraction of one unit cell, two Ti$-$O bonds are shortened a distance $\frac{1}{2}$, and eight Ba$-$(TiO_3) bonds are shortened $1/2\sqrt{3}$, which leads to the energy relationships $U=\frac{1}{4}k_s+\frac{1}{3}k_t=\frac{1}{2}c_{11}L$. The elastic constant c_{11} is thus

$$c_{11}=(1/L)(\tfrac{1}{2}k_s+\tfrac{1}{3}2k_t)=2.00\times10^{12}\text{ dynes/cm}^2,$$

in good agreement with the value $c_{11}=2.06\times10^{12}$ dynes/cm^2, determined experimentally.

Band Intensities

Information concerning the change in the electric dipole moment with interatomic distance can be obtained from the integrated intensity of infrared absorption bands. The change in dipole moment obtained for a normal vibration is the vector sum of the changes in dipole moments of the individual bonds. To determine this vector sum, the band intensities were measured for ν_1 and ν_2 for the powder spectra of $BaTiO_3$, $PbTiO_3$, $SrTiO_3$, $KNbO_3$, and $NaNbO_3$.

The extinction coefficient k is defined by $I_{\text{trans}}/I_{\text{inc}}=e^{-kx}$, where I is the intensity of the radiation and x is the path length. It can be shown, for the case of a system of gas molecules, that the integrated absorption intensity is[24]

$$\bar{k}=\int k(\nu)d\nu=\frac{8\pi^3N}{3ch}[(M)^{n,m}]^2,$$

where N is the number of molecules per unit volume, ν is the frequency, c the velocity of light, h Planck's constant, and $(M)^{n,m}=\int\psi_n\mu\psi_m^*d\tau$ the matrix element corresponding to the electric dipole transition between the states m and n. By expanding this transition moment in a power series in the normal coordinate q, and using the harmonic oscillator approximation, the change in electric dipole moment with normal coordinate distance is[3]

$$(dM/dq)^2=(3mc^2/\pi Nx)\bar{k}x.$$

Band areas from the powder data of Figs. 6 and 11 have been used. Since the low-frequency edge of band ν_2 could not be measured in most cases, the area under this band was determined from the curve half-width areas and the band shape. The normal vibrations are not pure bending or stretching vibrations; the reduced mass used was that satisfying the energy and momentum relationships for the normal motions computed from the force constants. Table VI shows the values of $|dM/dq|$ for $BaTiO_3$, $PbTiO_3$, $SrTiO_3$, $KNbO_3$, and $NaNbO_3$, for vibrations ν_1 and ν_2. In addition, the effective charge of the vibrating system was determined by the relationship $Q=|dM/dq|/\sqrt{3}\epsilon$, where ϵ is the electronic charge. Since the vibrations are triply degenerate, the factor of $\sqrt{3}$ must be included to yield the correct value for a single axis.

It is possible in theory to extend these calculations to separate the vector sum of $|dM/dq|$ computed above,

TABLE VI. Band intensities and derived constants.

Compound	Fundamental	$-kx$	Nx cm^{-2}	m (atomic mass units)	$\lvert dM/dq\rvert$ (esu) cm^{-2}	$Q(\epsilon)$
$BaTiO_3$	ν_1	269	1.48×10^{18}	5.8	1.23×10^{-9}	1.44
	ν_2	203	1.48	10.6	1.44	1.73
$PbTiO_3$	ν_1	362	1.74	5.8	1.32	1.57
	ν_2	118	1.74	12.3	1.10	1.32
$SrTiO_3$	ν_1	253	0.99	5.9	1.47	1.76
	ν_2	125	0.99	13.4	1.56	1.87
$KNbO_3$	ν_1	253	1.06	9.2	1.77	2.12
	ν_2	57	1.06	20.2	1.25	1.50
$NaNbO_3$	ν_1	262	1.10	9.3	1.78	2.14
	ν_2	39	1.10	20.2	1.02	1.22

[23] F. M. Seitz, *Modern Theory of Solids* (McGraw-Hill Book Company, Inc., New York, 1940), pp. 94 ff.

[24] R. S. Mulliken, J. Chem. Phys. **7**, 14 (1939).

to determine the individual change in dipole moment for each bond taking place in the normal vibration. This extension will not be made here, since the results of such a calculation are strongly dependent on the exact form of the normal vibrations, known only approximately because of the simplifying assumptions made in calculating the force constants.

The values obtained for $|dM/dq|$ are similar for all of the perovskite materials investigated, and are close to the values found by Waldron[3] for various ferrites, where the normal vibrations are also primarily those of oxygen ions. Since the values for the change in dipole moment obtained for $BaTiO_3$ is no larger than that obtained for these other nonferroelectric materials, there is no abnormally large effective charge in $BaTiO_3$ for the vibrations in the region investigated.

Single-Crystal Spectra

A discussion of the infrared spectrum of $BaTiO_3$ up to this point has dealt with the expected normal vibrations of the unit cell, and the use of these vibrational frequencies to determine the interatomic force constants, the vibrational specific heat contributions, and band intensities. In these discussions and computations, the slight departure of the lattice from the cubic perovskite structure has been ignored. The effect on the spectrum of the symmetry changes occurring at the various phase transitions will now be discussed.

The comparison of primary interest is that of the cubic and tetragonal spectra, since the material becomes ferroelectric when it undergoes the transition to the tetragonal state. The slightly broader band in the tetragonal spectrum (Fig. 3) is expected since this band is now doubly rather than triply degenerate. The band intensities are equal for the two phases. This indicates that the frequency difference between vibrations parallel and at right angles to the polar axis is slight; if one of the components of the tetragonal band experienced a large frequency change at the transition, it would shift out of the range of observation and the tetragonal band intensity would decrease markedly. Measurements of the maximum absorption while the temperature was slowly lowered through the Curie point indicate no anomalous intensity jump unexplainable by the slight shift of band center; this indicates that there is no radical change in the dipole moment with interatomic separation at the transition point.

The polarized-light measurements on the tetragonal crystal (Fig. 4) show that the vibrational frequency along the polar axis is about 20 cm^{-1} higher than that at right angles to the polar axis. Since the unit cell is about 1% longer along the polar axis, this seems to violate the general rule that the vibrational frequency decreases when the bond distance is increased. As shown by x-ray and neutron-diffraction measurements, the Ti ion is displaced in the tetragonal phase to a noncentral position in the oxygen octahedron, so that there are two $Ti-O_I$ distances of 1.87 and 2.17 A along the polar axis, as compared to the $Ti-O_{II}$ distance of 1.997 A at right angles to the polar axis.

The force constant, the second derivative of the potential energy with respect to internuclear separation, receives its major contribution from short-order, closed-shell repulsive forces rather than from Coulomb-attractive forces at the ionic equilibrium positions. The force constant will therefore be more sensitive to a decrease of bond length than to an increase, and although there is a net increase in the average bond distance along the polar axis when $BaTiO_3$ becomes tetragonal, the greater effect of decreasing one bond increases the over-all force constant and thus the vibrational frequency. The Ti—O distance at right angles to the polar axis is practically the same as the Ti—O distance of 2.004 A in the cubic phase. The fact that the same vibrational frequency of 495 cm^{-1} has been observed for each of these vibrations indicates that no large rearrangement of charge takes place at right angles to the polar axis when $BaTiO_3$ becomes tetragonal.

The symmetry arguments advanced earlier predicted that the band degeneracy should be completely removed in the orthorhombic phase and that the band should be tripled. However, two of the unit-cell dimensions are practically the same, and the slight frequency difference between these vibrations cannot be resolved. The rhombohedral band has the same double degeneracy as the tetragonal band, and a double absorption band is observed as expected.

The explanation of the observed low-temperature spectra on the basis of the change in symmetry properties is strengthened by the distinct changes in spectra near temperatures where phase transitions are known to occur, and by the absence of changes in band shape and intensity in the low-temperature spectrum of hexagonal barium titanate, prepared from the same starting materials as the perovskite form.

The infrared spectrum of barium titanate in the region investigated can thus be explained on the grounds of crystal symmetry and known atomic positions if intensity complications caused by different possible domain orientations are taken into account; nothing has been observed which can be related directly to ferroelectric effects.

Effect of Cation Replacement

Since the spectra of single crystals have been measured only for $BaTiO_3$ and $PbTiO_3$, a comparison of the spectra, to determine the effect of cation substitution, will deal primarily with the pressed-disk measurements, where the spectra could be measured under the same conditions for each material. The cation substitution may be expected to cause spectral changes due to alterations in unit-cell size, crystal structure, and binding energy.

The qualitative similarity of the powder spectra of $BaTiO_3$, $SrTiO_3$, $PbTiO_3$, and $CaTiO_3$ is expected in

TABLE VII. Vibration bands, band widths, and unit-cell dimensions for $SrTiO_3$, $BaTiO_3$, and $PbTiO_3$.

Material	ν_1 cm^{-1}	Band width ν_1 cm^{-1}	ν_2 cm^{-1}	Band width ν_2 cm^{-1}	c axis A	a axis A	Ti−O distance A
$SrTiO_3$	610	145	395	130	3.897	3.897	1.948
$BaTiO_3$	545	160	400	125	4.034	3.994	1.87[a]
$PbTiO_3$	590	215	405	150	4.152	3.90	1.79[a]

[a] The shorter Ti−O distance along the polar axis (c axis) is listed.

view of the assignment of the observed vibration bands to normal vibrations of the TiO_6 octahedron. The observed band locations can be explained by an inverse relationship between atomic separation and vibrational frequency, and the band widths by the degree of degeneracy of the band and the resulting departure from cubic symmetry (Table VII). $SrTiO_3$ is cubic, and band ν_1 is narrower than this band in the tetragonal materials $BaTiO_3$ and $PbTiO_3$. The band widths of $BaTiO_3$ and $PbTiO_3$ are about 15 cm^{-1} and 60 cm^{-1} greater, respectively, than that of $SrTiO_3$, about the separations observed between the two components of this band from single-crystal measurements (Figs. 4 and 8). It has been impossible to determine fine structure in band ν_2 for these materials; however, it can be seen that this band in $BaTiO_3$ and $PbTiO_3$ is less symmetric than in $SrTiO_3$.

In the ilmenite structure exhibited by $MgTiO_3$, $ZnTiO_3$, and $CdTiO_3$, the oxygen atoms are arranged in a warped hexagonal close packing, with one-third of the interstices filled with Mg atoms, one-third with Ti atoms, and one-third vacant.[25] Each Ti atom is surrounded by six O atoms, as in the perovskite modification, but the Ti−O chains present in the perovskite form no longer occur. In the observed spectra (Figs. 9 and 10), the band corresponding to the perovskite Ti−O stretching vibration is seen to be located in about the same position, although exhibiting much fine structure. The band corresponding to the low-frequency vibration ν_2 becomes doubled, due to the symmetry changes and the radically changed O−O repulsion forces.

The spectra of the orthorhombic perovskites $KNbO_3$ and $NaNbO_3$ (Fig. 11) are similar to that of orthorhombic $BaTiO_3$, with a shoulder on the low-frequency side of the high-frequency band ν_1, which adds weight to the assignment of the observed fine structure to symmetry effects. Since the vibrations ν_1 and ν_2 are primarily motions of oxygen ions, it is reasonable to expect that there is little difference between the titanate and niobate spectra. The niobate frequencies ν_1 are slightly higher than that for $BaTiO_3$, because of the smaller lattice size in these matrices[26] and the fact that the Nb atom has a higher charge than Ti, thus increasing the Nb−O force constant. Band ν_2 occurs at a frequency lower in the niobates than the titanates. The forces between oxygen and the monovalent cation K or Nb are less than the forces between oxygen and the divalent cations in the niobates. The low-frequency shoulder on band ν_1 is located about 100 cm^{-1} below the band center in $KNbO_3$ and about 150 cm^{-1} in $NaNbO_3$, compared to about 15 cm^{-1} in orthorhombic $BaTiO_3$. This is to be expected, since the orthorhombic $BaTiO_3$ structure is more nearly tetragonal than the orthorhombic niobates. The angles between the diagonals of the base of the orthorhombic unit cells are 90°8′ in $BaTiO_3$, 90°16′ in $KNbO_3$, and 90°40′ in $NaNbO_3$.[26]

$KNbO_3$ is ferroelectric at room temperature, while $NaNbO_3$ is antiferroelectric. In the ferroelectric arrangement, the slight atomic displacements from a symmetrical arrangement are in the same direction in all unit cells; in the antiferroelectric arrangement, neighboring cells have displacements in opposite directions. No differences between the spectra of $KNbO_3$ and $NaNbO_3$ were present which could be related to this effect.

ACKNOWLEDGMENTS

The author is greatly indebted to Professor A. R. von Hippel for suggesting this problem, and for much helpful advice and encouragement. It is also a great pleasure to acknowledge the assistance and advice of Dr. Robert D. Waldron in all phases of this investigation.

The $BaTiO_3$ crystals used were kindly supplied by V. Sils, H. Bradt, and J. Smiltens of the Laboratory for Insulation Research; crystals of $PbTiO_3$, $NaNbO_3$, and $KNbO_3$ by the Bell Telephone Laboratories; and a crystal of $SrTiO_3$ by the National Lead Company.

The author wished to express his gratitude to the International Business Machines Corporation for support in the form of a fellowship, and to Dr. D. R. Young of the International Business Machines Corporation for helpful discussions.

[25] R. W. G. Wyckoff, *Crystal Structures* (Interscience Publishers, Inc., New York, 1951).

[26] P. Vousden, Acta Cryst. **4**, 373 (1951).